encit 2020

ABCM
Associação Brasileira de Engenharia e Ciências Mecânicas

18th Brazilian Congress of Thermal Sciences and Engineering
November 16–20, 2020 (Online)

ENC-2020-0299
Validation of numerical modeling to evaluate the permeability of polymeric porous samples obtained by additive manufacturing

Ricardo Leite Martins Bazarin
Research Center for Rheology and Non-Newtonian Fluids (CERNN), Federal University of Technology - Paraná (UTFPR), Curitiba, Brazil.
ricardoleitemartins@hotmail.com

Rodolpho Kades de Oliveira e Silva
Research Center for Rheology and Non-Newtonian Fluids (CERNN), Federal University of Technology - Paraná (UTFPR), Curitiba, Brazil.
rodolpho_kades@hotmail.com

Marcelo Okada Shigueoka
Mechanical Engineering Department (DAMEC), Federal University of Technology - Paraná (UTFPR), Curitiba, Brazil.
mshigueoka@gmail.com

Neri Volpato
Mechanical Engineering Department (DAMEC), Federal University of Technology - Paraná (UTFPR), Curitiba, Brazil.
nvolpato@utfpr.edu.br

Silvio Luiz de Mello Junqueira
Research Center for Rheology and Non-Newtonian Fluids (CERNN), Federal University of Technology - Paraná (UTFPR), Curitiba, Brazil.
silvio@utfpr.edu.br

Abstract. *In the present work, the permeability of polymeric porous media produced by additive manufacturing (AM) in scaffolding structure is analyzed experimentally, numerically and theoretically, according to the permo-porous properties of the medium. The three-dimensional polymeric porous media are characterized by elliptical filaments equally spaced and alternated between layers (scaffolding). In the numerical and theoretical approaches the representation of the porous media is done using the concept of representative elementary volume (REV). In the experimental study the manufactured samples permeability was obtained using a steady-state liquid permeameter. A satisfactory precision in comparing experimental, numerical and theoretical approaches was achieved. Finally, a correlation for the permeability is proposed.*

Keywords: *porous media, additive manufacturing, permeability*

1. INTRODUCTION

The analysis of fluid flow in porous materials is relevant to interpret and improve the performance of processes in many areas, such as in the oil industry, geology, environmental systems, biological tissues, and others. In the oil and gas sector, specifically, the collection and characterization of porous samples from the reservoir are essential for several studies related to the oil recovery process. Given that collecting many samples from the formation is a costly process (McPhee *et al.*, 2015), an alternative to overcome this is to produce samples that allow mimicking the hydraulic properties such as porosity, permeability, and also pore diameters and wettability of the porous rocks present in the substrate.

In the literature, the additive manufacturing (AM) process has gained prominence in the production of porous media. once it allows the construction of porous substrates made of different materials like ceramic and polymers, with relatively low costs. With the rapid advance in the AM prototyping technique, the geometric freedom and improved control allow the fabrication of complex geometries that are sometimes impossible to get by other manufacturing processes (Volpato and Carvalho, 2017). Concerning the production of polymeric and ceramic materials, the material extrusion provided by the AM technique enables obtaining porous samples where the fibers are distributed in a scaffolding structure, as shown in Figure 1(a). The works of Too *et al.* (2001); Zein *et al.* (2002); Kalita *et al.* (2003); Chin Ang *et al.* (2006); Moroni *et al.* (2006); Dias *et al.* (2012); Blanquer *et al.* (2017) stand out among the various studies that explored the AM technique to

produce porous polymeric structures.

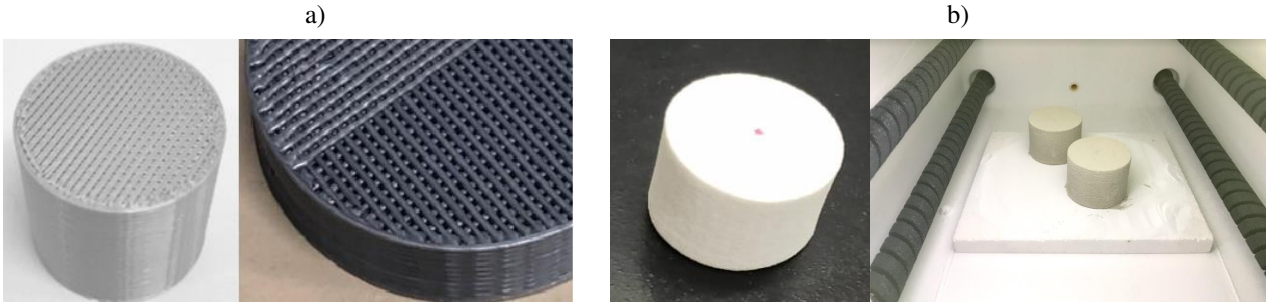

Figure 1. Porous samples produced by the AM process: a) polymeric sample, b) ceramic sample.

In the present work, one uses numerical, experimental, and theoretical approaches to characterize fibrous media produced by AM processes by obtaining properties such as permeability and porosity. To numerically simulate the fluid flow through the porous medium, one uses the finite volume method (FVM). A gas-based porosimeter and a liquid-based steady-state permeameter assist in the experimental characterization of the manufactured samples. Also, the theoretical part of the study uses the scale analysis technique to obtain a correlation for permeability. Finally, results show the comparison of the experimental permeability values with the numerical results and a correlation to validate the numerical model and verify the theoretical approach is presented.

2. PROBLEM FORMULATION

The AM prototyping process of fibrous porous media, represented in Figure 2, is characterized by a scaffold structure where the fibers are evenly spaced and rotated by 90^o per layer. The Figure 2 (a) shows the elliptical shape of the cross-section of the deposited fibers, with dimensions $a = 0.22mm$ and $b = 0.15mm$ being, respectively, the vertical and horizontal radius measurements.

In numerical and theoretical modeling, using the concept of representative elementary volume (REV) not only simplifies the geometry but also avoids high computational costs and complex boundary conditions. Accordingly, the three considerations allow the application of the REV concept to avoid the loss of representativeness of the geometry: the length of the fiber must be much greater than its thickness, i.e. $l_s >> b$, where l_s is the sample fiber length; the space between the fibers centers (S) must be much less than the fiber length, i.e. $l_s >> S$; the sample height (h_s) must be much greater than the length of the REV (l_{REV}), i.e., $h_s >> l_{REV}$. In this way, disregarding the wall effects, one can assume the porous medium as infinitely extensive. Figure 2 (a) shows the geometry of the REV and its relationship with the periodicity of the scaffolding structure that represents the porous sample.

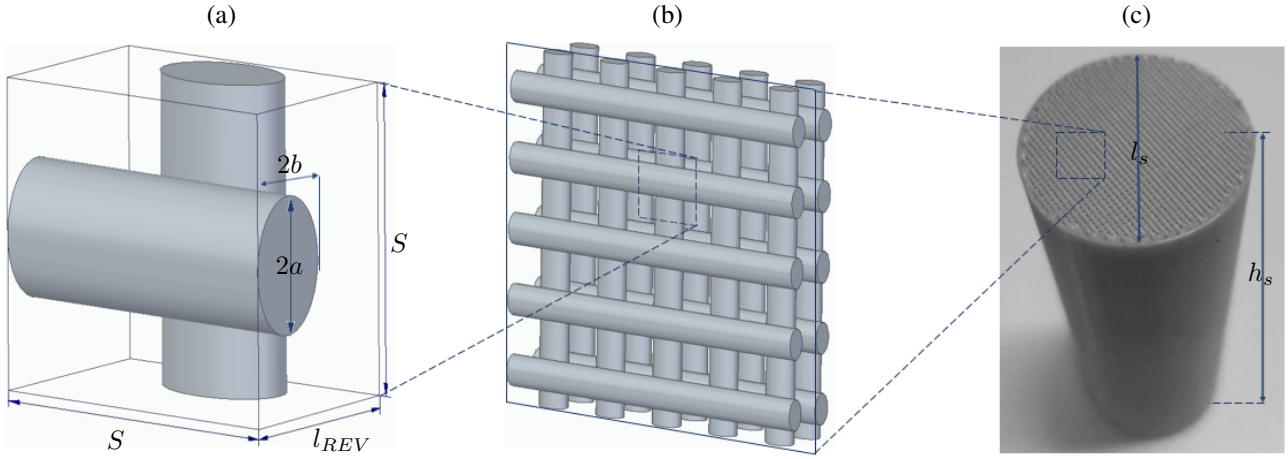

Figure 2. Representations of the polymeric porous media: a) REV, b) scaffolding structure, c) real sample.

The dimensional balance equations of mass and momentum that model the problem are expressed, respectively, as:

$$\frac{\partial \rho}{\partial t} + \nabla_{\boldsymbol{x}}(\rho \boldsymbol{u}) = 0, \tag{1}$$

$$\frac{\partial(\rho \boldsymbol{u})}{\partial t} + \nabla_{\boldsymbol{x}} \cdot (\rho \boldsymbol{u}\boldsymbol{u}) = -\nabla_{\boldsymbol{x}} p + \frac{1}{2}\nabla_{\boldsymbol{x}} \cdot \left[\mu\left(\nabla_{\boldsymbol{x}} \boldsymbol{u} + \nabla_{\boldsymbol{x}} \boldsymbol{u}^T\right)\right] + \rho \boldsymbol{g}. \tag{2}$$

The dimensional quantities used in the equations (1) and (2) are the three coordinates (x, y, z), the corresponding velocity vector components (u, v, w), the density ρ, the pressure p, the dynamic viscosisty μ, the time t and the external force vector per unit of mass $\boldsymbol{g}$. The boundary conditions for the problem are non-slip condition on the solid surfaces, periodic boundary condition on all boundaries of the REV and constant pressure drop in perpendicular direction to the fibers axis. For a newtonian fluid, the flow is assumed incompressible and isothermal, gravitational and the inertial forces are neglected (Darcy Regime), and the flow is assumed in steady-state regime. Based on the hypothesis, the Equation (2) can be written in the form of the Stokes equation:

$$\mu \nabla^2_{\boldsymbol{x}} \boldsymbol{u} = \nabla_{\boldsymbol{x}} p, \tag{3}$$

The permeability in the present work is determined by the Hazen-Darcy equation, given by:

$$U_{Da} = \frac{K}{\mu}\frac{dp}{dx}. \tag{4}$$

where U_{Da} is the Darcy velocity, which represents mean velocity in the x direction (Lage, 1998). The fibrous porous media porosity (ϕ), which represents the fraction of the total volume of the medium that is occupied by voids, is written by:

$$\phi = 1 - \frac{V_{sol}}{V_T} = 1 - \frac{2\pi abS}{S^2 4b} = 1 - \frac{\pi a}{2S} \tag{5}$$

where V_{sol} is solid volume and V_T is total volume of the sample.

For the experimental approach, samples prototyped by polymeric fibers are used, as illustrated in Figure 2 c). The values of spacing between fibers centers, height, diameter, weight (W), volume of solid, theoretical porosity (CAD design), measured porosity and the percentual deviation between the measured and theoretical porosity of each sample are shown in Table 1. The porosity measurement was made by a helium gas porosimeter using a grain volume procedure, for more details of the procedure see McPhee *et al.* (2015).

Table 1. Comparison of real foams and modeled structures

Sample	$S(mm)$	$h_s(mm)$	$l_s(mm)$	$W(g)$	$V_{sol}(ml)$		ϕ		
					W/ρ	Posimeter	CAD	Porosimeter	deviation (%)
1	0.61	72	25	30.14	21.32	21.08	0.4338	0.3538	22.61
2	0.66	72	25	27.51	19.32	19.23	0.4767	0.4155	14.72

3. NUMERICAL, THEORETICAL AND EXPERIMENTAL PROCEDURE

3.1 Finite-Volume Method

The numerical approach in this work is used to determine the permeability property, where the Finite-Volume method (FVM) is applied in the flow simulation through the porous media represented by the REV. The flow is discretized in several control volumes that gives form to a mesh, the SIMPLE algorithm is used for the velocity-pressure coupling and the QUICK scheme is used for the discretization of the Navier-Stokes equation. For more details on the SIMPLE algorithm and the QUICK scheme see Versteeg and Malalasekera (2007). The FVM allows unstructured meshes for the problem, which presents some advantages such as: they are easier to be formulated, results in less computational time in comparison to structured meshes and allows the CAD design of porous medium with exact values of porosity.

3.2 Scale Analysis Technique

The scale analysis technique consists of a theoretical approach that allows the interpretation of basic characteristics of the problem by estimating scales for the terms present in the governing equations (Bejan, 1985; Clague *et al.*, 2000). In order to estimate the permeability values, the scale analysis allows to obtain a correlation according to properties of the porous medium and adjustment coefficients. In the present work the applied scale analysis technique follows the formulation proposed by Tamayol and Bahrami (2011).

Based on the governing equations of the problem and their hypotheses, one assumes a flow where the inertial forces are negligible in relation to the viscous ones, therefore characterizing a Darcy regime, where Equation (4) is valid. Applying the scale analysis on the left side of the Equation (3), the pressure gradient scale is obtained:

$$\tilde{U}\frac{\mu}{\delta_{min}^2} \approx \frac{dp}{dx}, \tag{6}$$

where $\tilde{U}$ is the pore-scale velocity and δ_{min} the radius of the smallest pore of the geometry. Due to the homogeneous structure of the porous medium the radius of the smallest pore can be easily determined for each porous medium configuration, where

$$\delta_{min} = \frac{(S-2a)}{2} = \frac{\pi a}{4(1-\phi)} - a = a\left[\frac{\pi}{4(1-\phi)} - 1\right]. \tag{7}$$

Based on the works of Clague *et al.* (2000) and Sobera and Kleijn (2006), Tamayol and Bahrami (2011) propose the velocity scale at the pore level, given by:

$$\tilde{U} \approx \frac{U_{Da}}{T\phi}. \tag{8}$$

Replacing the Equations (4) and (8) in the Equation (6), yields:

$$K = C_0\phi\delta_{min}^2 T, \tag{9}$$

where C_0 is the adjustment constant to be determined and T is the tortuosity represented in present case by Archie's equation (Archie *et al.*, 1942):

$$T = \left(\frac{1}{\phi}\right)^{\alpha} \tag{10}$$

where α is another adjusment constant. Therefore, replacing the Equations (7) and (10) in Equation (9) there is a correlation for permeability of the porous media proposed in the form

$$K = C_0\phi^{(1-\alpha)}a^2\left[\frac{\pi}{4(1-\phi)} - 1\right]^2. \tag{11}$$

3.3 Steady-State Liquid Permeameter

In the experimental measurement of permeability, a steady-state liquid permeameter illustrated and detailed in Figure 3 is used. The experimental setup basically consists of two tanks, pump, coreholder and a differential pressure trnsmitter. In the measurement process, the pump supplies the system with a constant flow rate of distilled water between 1 and 10 ml/min from tank 1 to tank 2, between the pump and tank 2 the fluid flows through the porous medium lodged longitudinally in the coreholder, while the fluid flows through the porous medium the differential pressure transmitter measures the difference in pressure between the outlet and inlet of the coreholder, which is collected digitally using a LabView Software of data acquisition. The measurement process ends when a stable pressure value is reached, which is considered a steady-state flow regime and the permeability can be calculated by the Equation (4) using $\mu = 0.0011\ Pa.s$ for distilled water .

4. RESULTS

4.1 Numerical Results

In order to ensure the numerical permeability, the finite volume method was applied in the flow simulation through the REV for different values of S that result in a variation of the porosity between 0.23 to 0.5, so that for the present geometry in $S = 0.44(mm)$ the porous medium reaches the limit porosity of $\phi = 1 - \pi/4$ where the fibers touch blocking the flow.

Considering the case of $\phi = 0.23$ as the critical case, a mesh sensitivity test is performed in order to obtain an adequate number of elements to simulate the problem. The number of elements in the mesh is controlled by the average element size. The test is given by calculating the permeability in an initial simulation with an arbitrary number of elements, subsequently the number of elements is doubled and the calculated permeability is compared with the permeability of the previous mesh. This duplication process is repeated until the percentage difference EK between the permeabilities reaches a value less than 10%. In Table 2, the mesh sensitivity test is exemplified and the values obtained for the case $\phi = 0.23$ are presented, in which the mesh number 4 was chosen.

Defined the reference mesh based on the critical case, the simulations are applied to the porosities $\phi = 0.5$, 0.45, 0.4, 0.35, 0.3, 0.25, 0.24 and 0.23. In the Figure 4 are illustrated the streamlines for each of the simulated cases. The permeability values obtained for each case are presented and compared in Figure 6 and Table 3.

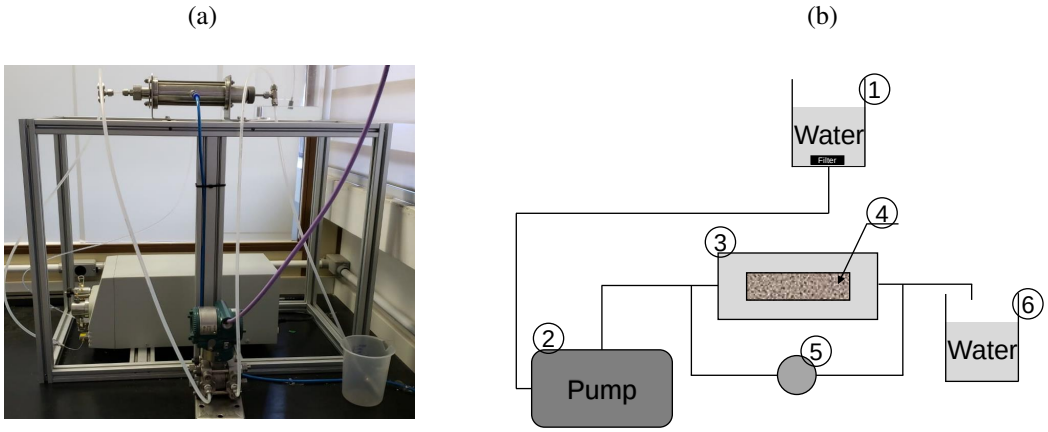

Figure 3. Steady-state liquid permeameter: (a) experimental setup for measuring permeability; (b) Schematic diagram of the experimental setup: (1) tank 1, (2) pump, (3) coreholder, (4) porous media, (5) differential pressure transmitter, and (6) tank 2.

Table 2. Mesh sensivity test for $\phi = 0.23$.

Mesh	Average element size (mm)	Number of elements	$K(mD)$	$EK(\%)$
1	45.0×10^{-3}	19041	3.16734×10^{3}	31.28
2	33.3×10^{-3}	38365	2.41272×10^{3}	27.32
3	24.4×10^{-3}	76373	1.89498×10^{3}	15.32
4	18.0×10^{-3}	151485	1.64325×10^{3}	9.73
5	13.2×10^{-3}	300733	1.49755×10^{3}	-
$EK = (1 - K_i/K_{i+1}) \times 100$				

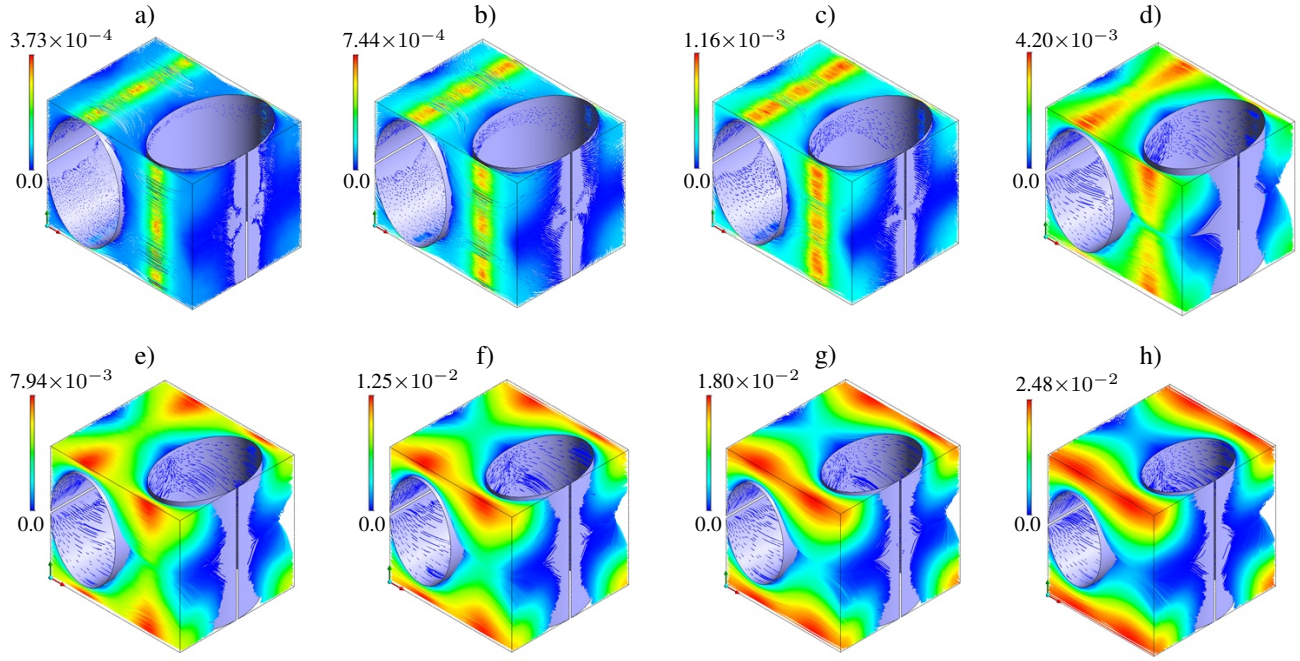

Figure 4. Streamlines field of the fluid flow in REV for: a) $\phi = 0.23$, b) $\phi = 0.24$, c) $\phi = 0.25$, d) $\phi = 0.30$, e) $\phi = 0.35$, f) $\phi = 0.40$, g) $\phi = 0.45$ and h) $\phi = 0.50$. The color gradient in each case illustrate the velocity magnitude in the streamlines.

4.2 Correlation Adjustment

In the theoretical analysis presented in Subsection 3.2a permeability correlation (Eq. 11) is defined depending on two adjustment constants, i.e., α and C_0. The constant C_0 controls the vertical displacement (on the permeability axis) of

the correlation, which can be adjusted depending on both numerical and experimental permeability results. The second constant α related to the correlations of Archie *et al.* (1942) for tortuosity is constantly chosen from $1.2 \leq \alpha \leq 4.4$ in different formulations of porous media (Friedman, 2005), however Tamayol and Bahrami (2011) considers that $\alpha = 0.5$ provides a good estimate for a scaffold structure porous media. In the present work both constants are adjusted numerically in order to minimize the percentage difference in relation to the numerical permeability values, resulting in $\alpha = 0.951749$ and $C_0 = 0.099564$.

4.3 Experimental Results

As a procedure to obtain the experimental results, the $\Delta p - Q$ (pressure drop-volumetric flow rate) relationship is analyzed for each case in order to observe the Darcy regime behavior described by Equation (4). The results obtained for pressure drop due to the volumetric flow rate variation between 7 and 10 ml/min can be seen in Figure 5 for the two porous samples tested, noting an approximately linear behavior that indicates the flow in Darcy regime, in which the Equation (4) can be used to determine permeability. The final result of the sample permeability is determined by an average of the permeability calculated at each point of pressure drop, the dashed lines plotted in the Figure 5 illustrate the linear behavior of the permeability obtained for each sample. The permeability results for each tested sample are presented in Table 3 and in Figure 6 as a function of porosity for the CAD design porosity (Theoretical Porosity) and for the porosimeter measurements (Measured Porosity).

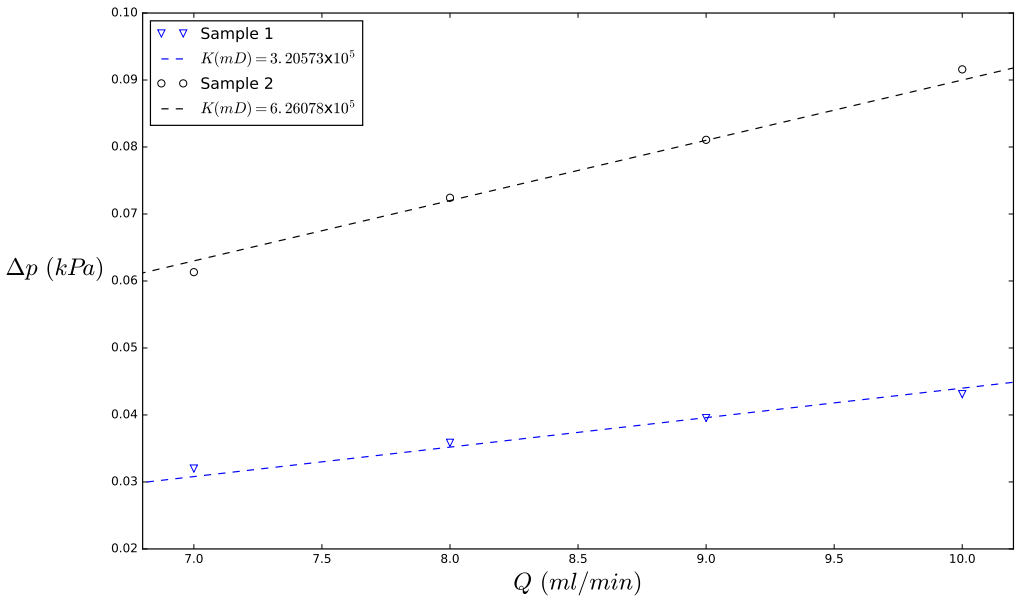

Figure 5. $\Delta p - Q$ behavior for measured 3D porous media.

4.4 Comparison Between Approaches

Discussed the specific characteristics and results of each approach, in this subsection the permeability values obtained are presented in milidarcy unit (mD) and compared both graphically and quantitatively. In Figure 6, the permeability-porosity relationship of the numerical and experimental results are plotted together with the correlation defined by the Equation (11). Visually, an excellent agreement is observed between the numerical results and the theoretical correlation, while the experimental results plotted according to the theoretical and measured porosity present relatively greater differences.

In a quantitative comparison, the permeability values are shown in Table 3 and compared point by point using percentage differences between permeability (EK). Comparing the theoretical correlation with the numerical results, an excellent precision is observed with a maximum percentage difference of $EK = 9.30\%$, however such proximity of the values are expected due to the correlation constants being adjusted based on the numerical results. In the comparison of the experimental results with the theoretical correlation, relatively larger percentage differences were observed than those presented in the numerical-correlation comparison, however a good approximation with a maximum percentage difference of $EK = 53.29\%$ can be considered. Additionally between the experimental results considering the measured and

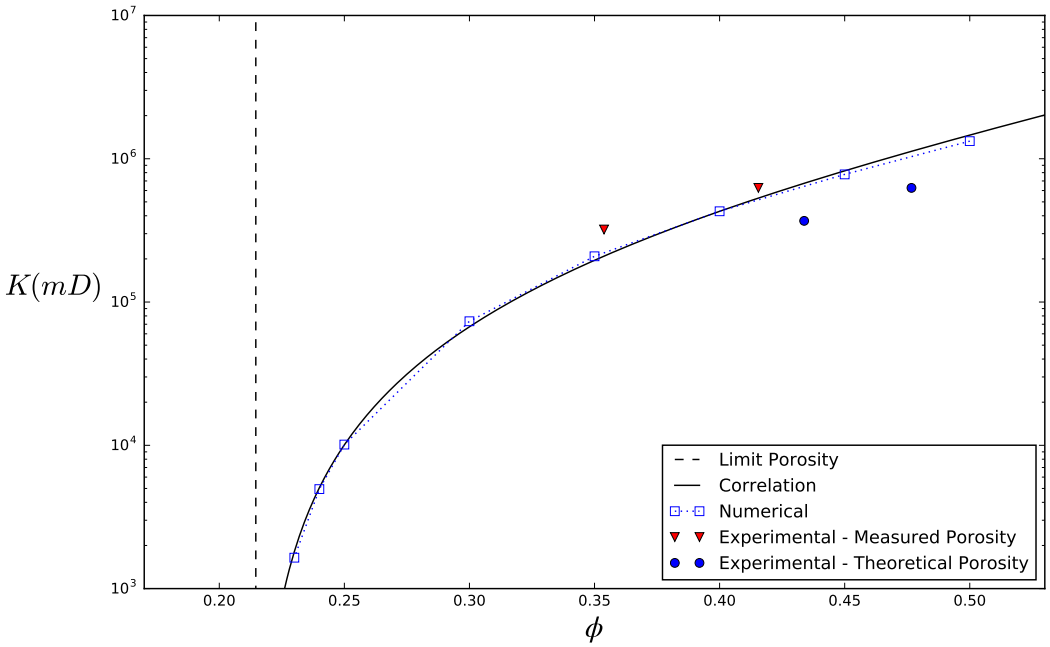

Figure 6. Permeability results as a function of porosity.

theoretical prosities, the percentage differences for the measured porosities demonstrate a greater proximity in relation to the theoretical correlation.

Table 3. Comparison between $K(mD)$ values for numerical, theoretical and experimental approaches.

ϕ	$K_{\text{Numerical}}$	$K_{\text{Correlation}}$	$EK_{(1)}$ [%]	$\phi_{\text{Theoretical}}$	$K_{\text{Experimental}}$	$K_{\text{Correlation}}$	$EK_{(2)}$ [%]
0.50	1.32699×10^6	1.46305×10^6	9.30	0.4767	6.26078×10^5	1.12704×10^6	44.45
0.45	7.77866×10^5	8.23495×10^5	5.54	0.4338	3.68559×10^5	6.74035×10^5	45.32
0.40	4.30027×10^5	4.29764×10^5	0.06	ϕ_{Measured}			
0.35	2.08591×10^5	1.95584×10^5	6.65	0.4155	6.26078×10^5	5.31532×10^5	17.79
0.30	7.34277×10^4	6.71961×10^4	9.27	0.3538	3.20573×10^5	2.09131×10^5	53.29
0.25	1.01193×10^4	1.00767×10^4	0.42				
0.24	4.94826×10^3	5.05413×10^3	2.09				
0.23	1.64325×10^3	1.81059×10^3	9.24				

$EK_{(1)} = (1 - K_{\text{Numerical}}/K_{\text{Correlation}}) \times 100$

$EK_{(2)} = (1 - K_{\text{Experimental}}/K_{\text{Correlation}}) \times 100$

5. CONCLUSIONS

In the present work, different approaches are used to estimate the permeability of polymeric porous media samples obtained by additive manufacturing technique has been presented. The scaffold structure of the polymeric porous media was analyzed using the finite-volume method and scale analysis applied to the flow conservation equations. Experimental results of porosity and permeability were obtained using a gas porosimeter and a steady-state liquid permeameter. In the analysis of the results, a satisfactory precision was observed comparing the numerical and experimental values of permeability with the theoretical correlation. Consequently, the theoretical correlation obtained by the scale analysis adequately represent the permeability behavior of manufactured porous media as a function of porosity. Therefore, the combination of the presented approaches demonstrates a good efficiency in the characterization of the permo-porous properties of porous polymeric media based on based on scaffolding structure.

6. ACKNOWLEDGEMENTS

The authors are thankful to the support provided by the research and development department of Repsol Sinopec Brasil. This project is a joint research effort of Repsol-Sinopec and UTFPR, developed with the ANP research and development incentive law number 9.478, 06/08/1997.

7. REFERENCES

Archie, G.E. *et al.*, 1942. "The electrical resistivity log as an aid in determining some reservoir characteristics". *Transactions of the AIME*, Vol. 146, No. 01, pp. 54–62.

Bejan, A., 1985. "The method of scale analysis: natural convection in porous media". *Natural Convection: Fundamentals and Applications*, Vol. 551, pp. 548–572.

Blanquer, S.B., Werner, M., Hannula, M., Sharifi, S., Lajoinie, G.P., Eglin, D., Hyttinen, J., Poot, A.A. and Grijpma, D.W., 2017. "Surface curvature in triply-periodic minimal surface architectures as a distinct design parameter in preparing advanced tissue engineering scaffolds". *Biofabrication*, Vol. 9, No. 2, p. 025001.

Chin Ang, K., Fai Leong, K., Kai Chua, C. and Chandrasekaran, M., 2006. "Investigation of the mechanical properties and porosity relationships in fused deposition modelling-fabricated porous structures". *Rapid Prototyping Journal*, Vol. 12, No. 2, pp. 100–105.

Clague, D., Kandhai, B., Zhang, R. and Sloot, P.M., 2000. "Hydraulic permeability of (un) bounded fibrous media using the lattice boltzmann method". *Physical Review E*, Vol. 61, No. 1, p. 616.

Dias, M., Fernandes, P., Guedes, J. and Hollister, S., 2012. "Permeability analysis of scaffolds for bone tissue engineering". *Journal of biomechanics*, Vol. 45, No. 6, pp. 938–944.

Friedman, S.P., 2005. "Soil properties influencing apparent electrical conductivity: a review". *Computers and electronics in agriculture*, Vol. 46, No. 1-3, pp. 45–70.

Kalita, S.J., Bose, S., Hosick, H.L. and Bandyopadhyay, A., 2003. "Development of controlled porosity polymer-ceramic composite scaffolds via fused deposition modeling". *Materials Science and Engineering: C*, Vol. 23, No. 5, pp. 611–620.

Lage, J., 1998. "The fundamental theory of flow through permeable niedia from darcy to turbulence". *Transport phenomena in porous media*, Vol. 1.

McPhee, C., Reed, J. and Zubizarreta, I., 2015. *Core analysis: a best practice guide*. Elsevier.

Moroni, L., De Wijn, J. and Van Blitterswijk, C., 2006. "3d fiber-deposited scaffolds for tissue engineering: influence of pores geometry and architecture on dynamic mechanical properties". *Biomaterials*, Vol. 27, No. 7, pp. 974–985.

Sobera, M. and Kleijn, C., 2006. "Hydraulic permeability of ordered and disordered single-layer arrays of cylinders". *Physical Review E*, Vol. 74, No. 3, p. 036301.

Tamayol, A. and Bahrami, M., 2011. "Transverse permeability of fibrous porous media". *Physical Review E*, Vol. 83, No. 4, p. 046314.

Too, M., Leong, K., Chua, C., Cheah, C. and Ho, S., 2001. "Feasibility of tissue engineering scaffold fabrication using fused deposition modelling". In *The Seventh Australian and New Zealand Intelligent Information Systems Conference, 2001*. IEEE, pp. 433–438.

Versteeg, H.K. and Malalasekera, W., 2007. *An introduction to computational fluid dynamics: the finite volume method*. Pearson education, 2nd edition.

Volpato, N. and Carvalho, J.d., 2017. "Introdução à manufatura aditiva ou impressão 3d". *Manufatura Aditiva–Tecnologias e aplicações da impressão D*, Vol. 3, p. 400.

Zein, I., Hutmacher, D.W., Tan, K.C. and Teoh, S.H., 2002. "Fused deposition modeling of novel scaffold architectures for tissue engineering applications". *Biomaterials*, Vol. 23, No. 4, pp. 1169–1185.

8. RESPONSIBILITY NOTICE

The authors are solely responsible for the printed material included in this paper.